

Structure, Microwave Dielectric Properties, and Low-Temperature Sintering of Acceptor/Donor Codoped $\text{Li}_2\text{Ti}_{1-x}(\text{Al}_{0.5}\text{Nb}_{0.5})_x\text{O}_3$ Ceramics

Tianwen Zhang, Ruzhong Zuo[†] and Jian Zhang

Institute of Electro Ceramics & Devices, School of Materials Science and Engineering, Hefei University of Technology, Hefei 230009, China

The structure, microwave dielectric properties, and low-temperature sintering behavior of acceptor/donor codoped Li_2TiO_3 ceramics [$\text{Li}_2\text{Ti}_{1-x}(\text{Al}_{0.5}\text{Nb}_{0.5})_x\text{O}_3$, $x = 0-0.3$] were investigated systematically. The x-ray diffraction confirmed that a single-phase solid solution remained within $0 < x \leq 0.2$ and secondary phases started to appear as $x > 0.2$, accompanied by an order-disorder phase transition in the whole range. Scanning electron microscopy observation indicated that the complex substitution of Al^{3+} and Nb^{5+} produced a significant effect on the microstructural morphology. Both microcrack healing and grain growth contributed to the obviously enhanced $Q \times f$ values. By comparison, the decrease of ϵ_r and τ_f values was ascribed to the ionic polarizability and the cell volume, respectively. Excellent microwave dielectric properties of $\epsilon_r \sim 21.2$, $Q \times f \sim 181\,800$ GHz and $\tau_f \sim 12.8$ ppm/°C were achieved in the $x = 0.15$ sample when sintered at 1150°C. After 1.5 mol% $\text{BaCu}(\text{B}_2\text{O}_5)$ additive was introduced, it could be well sintered at 950°C and exhibited good microwave dielectric properties of $\epsilon_r \sim 20.4$, $Q \times f \sim 53\,290$ GHz and $\tau_f \sim 3.6$ ppm/°C as well. The cofiring test of the low-sintering sample with Ag powder proved its good chemical stability during high temperature, which enables it to be a promising middle-permittivity candidate material for the applications of low-temperature cofired ceramics.

I. Introduction

Li_2TiO_3 ceramic with a rock salt structure was reported to have excellent microwave dielectric properties of $\epsilon_r \sim 22.14$, $Q \times f \sim 63\,500$ GHz, and $\tau_f \sim 20.3$ ppm/°C, when sintered at a relatively low temperature $\sim 1300^\circ\text{C}$.¹ With the increment of firing temperature, it would change from a metastable α -phase to a disordered γ -phase gradually. Simultaneously, there occurs an order-disorder phase transition at 1215°C.^{2,3} Since the typical mean bond length of Li–O (2.14 Å) is longer than that of Ti–O (1.95 Å), the Li–O bonds are weaker.⁴ These two aspects have become main reasons for the easy cleavage on (001) plane, which further leads to the generation of microcracks. It was considered as the main obstacle for obtaining a pure and dense Li_2TiO_3 ceramic in addition to the volatilization of lithium at high temperature. The addition of low-melting-point additives^{5,6} could lower its densification temperature, yet impurities generally tended to deteriorate the microwave dielectric properties. On the other hand, the 0.76 Li_2TiO_3 –0.24 MgO ceramics⁷ were found to have optimum microwave dielectric properties of dielectric constant $\epsilon_r \sim 19.2$, quality factor $Q \times f \sim 106\,226$ GHz, and the temperature coefficient of reso-

nant frequency $\tau_f \sim 3.56$ ppm/°C. The improvement of $Q \times f$ value was ascribed to both the alleviation and disappearance of cleavage on (001) plane and the stabilization of ordering-induced domain boundaries by partial segregation of Mg. A similar modification mechanism was also reported in the ceramics of $\text{Ba}(\text{Zn}_{1/3}\text{Ta}_{2/3})\text{O}_3$ – BaZrO_3 and $(1-x)\text{Li}_2\text{TiO}_3$ – $x\text{ZnO}$.^{8,9} Moreover, the microwave dielectric performance of Li_2TiO_3 was improved by substituting complex ion $(\text{Zn}_{1/3}\text{Nb}_{2/3})^{4+}$ for Ti^{4+} .¹⁰

It is known that most titanate-based materials often suffered from the oxygen loss as sintered at high temperatures, which might partially reduce Ti^{4+} to Ti^{3+} and further increase the dielectric loss.^{11,12} A traditional way to improve this situation is to fire the samples in a high-oxygen-partial-pressure atmosphere. By comparison, a more convenient and effective way should be to add a few acceptor dopants. Pullar et al. had successfully suppressed the reduction of Ti^{4+} in the TiO_2 matrix by adding small amounts of acceptor ions, such as Al^{3+} , Mg^{2+} , and Zn^{2+} .¹³ In addition, introduction of a few donor ions seemed to work as well in some materials. For instance, Kuang et al. had improved the $Q \times f$ value of MgTiO_3 ceramic via a small amount Ta^{5+} doping.¹⁴

Based on the above considerations, Al_2O_3 as a dopant was for the first time introduced into the Li_2TiO_3 ceramic in this work. Except for its role as acceptor dopant, an appropriate amount of Al_2O_3 was also beneficial for the growth and uniformity of the ceramic grains.¹⁵ Moreover, to stabilize the monoclinic structure and keep the charge balance, we have also introduced Nb^{5+} to form the complex $(\text{Al}_{0.5}\text{Nb}_{0.5})^{4+}$ ions for replacing Ti^{4+} ions. Excellent microwave dielectric properties in CaTiO_3 ceramic were obtained after substituting $(\text{Al}_{0.5}\text{B}_{0.5})^{4+}$ (B=Nb, Ta) for Ti^{4+} ions.^{16,17} Moreover, the similar ionic radius between $(\text{Al}_{0.5}\text{Nb}_{0.5})^{4+}$ (0.586 Å) and Ti^{4+} (0.605 Å)¹⁸ would make the substitution process feasible in theory in despite of different crystal structures between Li_2TiO_3 and CaTiO_3 . The sintering behavior, structural evolution, and microwave dielectric properties of $\text{Li}_2\text{Ti}_{1-x}(\text{Al}_{0.5}\text{Nb}_{0.5})_x\text{O}_3$ ($x = 0-0.3$) ceramics were investigated in detail. To further meet the requirements of low-temperature cofired ceramic (LTCC) technology, $\text{BaCu}(\text{B}_2\text{O}_5)$ (BCB) was selected as a sintering aid due to its low-melting point ($\sim 850^\circ\text{C}$) and favorable microwave dielectric properties of $\epsilon_r \sim 7.4$, $Q \times f \sim 50\,000$ GHz, and $\tau_f \sim -32$ ppm/°C.¹⁹

II. Experimental Procedure

The $\text{Li}_2\text{Ti}_{1-x}(\text{Al}_{0.5}\text{Nb}_{0.5})_x\text{O}_3$ ($x = 0-0.3$) and BCB ceramic powders were both synthesized through a conventional solid-state reaction method. High-purity ($>99.9\%$) powders of Li_2CO_3 , TiO_2 , Al_2O_3 , and Nb_2O_5 were used as the raw materials to synthesize $\text{Li}_2\text{Ti}_{1-x}(\text{Al}_{0.5}\text{Nb}_{0.5})_x\text{O}_3$ according to the stoichiometric ratio, and the mixtures were ground by planetary ball milling for 4 h in the alcohol medium using zirconia balls. The slurries were dried, calcined at 800°C – 850°C for 2 h, and then remilled for 6 h again. The BCB powder was prepared via mixing the high-purity ($>99.9\%$) Ba

N. Alford—contributing editor

Manuscript No. 36589. Received March 17, 2015; approved November 5, 2015.

[†]Author to whom correspondence should be addressed. e-mails: piezolab@hfut.edu.cn and rzuo@hotmail.com

(OH)₂·8H₂O, CuO, and B₂O₃ powders. After being calcined at 800°C for 2 h, it was then mixed with the Li₂Ti_{0.85}(Al_{0.5}Nb_{0.5})_{0.15}O₃ powder according to the formula of Li₂Ti_{0.85}(Al_{0.5}Nb_{0.5})_{0.15}O₃ + *y* mol% BCB (*y* = 0.5, 1.0 and 1.5). The powder mixtures were added with 5 wt% poly vinyl alcohol (PVA) as a binder and subsequently pressed into cylinders with dimensions of 10 mm in diameter and 7–8 mm in height. The Li₂Ti_{1-x}(Al_{0.5}Nb_{0.5})_xO₃ (*x* = 0–0.3) specimens were sintered in the temperature range of 1000°C–1250°C for 2 h in air. And the BCB-added specimens were sintered at 900°C–1000°C for 2 h. In order to suppress the lithium evaporation loss, the specimens were muffled with the powders of the same composition. The bulk densities of the sintered pellets were measured by the Archimedes method.

The crystal structure of the sintered ceramics was examined by an X-ray diffractometer (XRD, D/Max2500 V, Rigaku, Japan) using CuK α radiation. The Raman experiments were carried out for the sintered samples at room temperature using a Raman microscope (532 nm, LabRam, HR Evolution; HORIBA JOBIN YVON, Kyoto, Japan). The grain morphology was analyzed by a scanning electron microscope (SEM, JSM-6490LV; JEOL, Tokyo, Japan) equipped with an energy dispersive spectrometer (EDS). Microwave dielectric properties of the sintered samples were measured by a network analyzer (N5230C; Agilent, Palo Alto, CA) in the frequency range of 6–10 GHz. The dielectric constant was measured by the Hakki–Coleman method²⁰ modified by Courtney, and the unloaded *Q* values were measured by the cavity method.²¹ The τ_f value of the samples was measured in the temperature range from 20°C to 80°C.

III. Results and Discussion

The XRD full patterns of the Li₂Ti_{1-x}(Al_{0.5}Nb_{0.5})_xO₃ (*x* = 0–0.3) ceramics sintered at optimal temperatures for 2 h are exhibited in Fig. S1. A rock-salt monoclinic phase was identified as the main phase according to the standard pattern of Li₂TiO₃ phase (JCPDS #33-0831). No secondary phases were detected until the *x* value was more than 0.2. Some tiny peaks corresponding to the Al₂O₃ (JCPDS #10-0414) and Nb₂O₅ (JCPDS #43-1042) phases appeared when *x* = 0.25 and 0.30, which might be attributed to the solubility limit of Li₂TiO₃ phase. Of particular note was that the long-range ordering degree of cations decreased with increasing the (Al_{0.5}Nb_{0.5})⁴⁺ content, as indicated by the decreasing (002) peak intensity and increasing (–133) peak intensity, as described in Figs. 1(a) and (b), respectively, suggesting an order-disorder phase transition. As mentioned above, we assumed that the (Al_{0.5}Nb_{0.5})⁴⁺ substituted for Ti⁴⁺ in Li₂TiO₃. As a result, the cell volume of the matrix composi-

tion should become small within the solubility range due to smaller sizes of (Al_{0.5}Nb_{0.5})⁴⁺ than Ti⁴⁺. However, it increased with increasing *x*, as confirmed by the fact that the (–133) peak moved toward to lower angles (see Fig. S1). The detailed cell volume data inside the solubility limit were given in the forthcoming section.

The Raman spectra of the Li₂Ti_{1-x}(Al_{0.5}Nb_{0.5})_xO₃ (*x* = 0–0.3) ceramics are shown in Fig. 2. As 0.05 ≤ *x* ≤ 0.2, the specimens exhibited almost the same Raman spectra as that of pure Li₂TiO₃ ceramic, suggesting that the solid solution was formed. As more (Al_{0.5}Nb_{0.5})⁴⁺ content was added, a new band at 797 cm^{–1} started to appear and its intensity increased. A similar phenomenon could also be observed in the system of Li₂TiO₃–LiF²² in which the appearance of the new band (825 cm^{–1}) was ascribed to the relaxations of selection rules by the decrease of crystal symmetry at the short range ordering domain boundaries as a result of the break of the translational symmetry of crystalline materials. Since a large number of modes were overlapped or interacted, it was not easy to distinguish and assign all of the modes from the Raman spectra. According to the literature,²³ bands in the region of 700–500 cm^{–1} should be assigned to the Ti–O stretching vibrations, bands in the region 420–400 cm^{–1} should be labeled as Li–O stretching vibrations, and those in the region 350–250 cm^{–1} could be marked as Li–O stretching vibrations and O–Li–O bending vibrations. The O–Ti–O and O–Li–O bending vibrations appeared in the region 350–320 cm^{–1}. It should be noted that some obvious Raman peaks, i.e., bands at 350, 402, 418 and 656 cm^{–1}, presented a slight broadening with increasing *x*, which might be ascribed to the decrease of the cation ordering.

The typical SEM images of the Li₂Ti_{1-x}(Al_{0.5}Nb_{0.5})_xO₃ (*x* = 0–0.3) ceramics sintered at optimal temperatures for 2 h are depicted in Fig. 3. A porous and uneven microstructure with microcracks (marked by the arrows) emerged in the pure Li₂TiO₃ ceramic sintered at 1200°C, as presented in Fig. 3(a). The characteristic microcracks were usually considered as the main reason why pure Li₂TiO₃ ceramics were hardly sintered well at high temperatures. Moreover, the grain morphology was found to change dramatically from an irregular plate shape into a round shape as *x* = 0.05, and at the same time, the specimen tended to be dense, accompanied by the disappearance of microcracks and the decrease of grain size. Obviously, the microstructure of the specimens became more homogeneous with increasing *x*. However, more (Al_{0.5}Nb_{0.5})⁴⁺ substitution tended to promote the grain growth, reaching the maximum value of ~4.8 μm in average in the dense Li₂Ti_{0.85}(Al_{0.5}Nb_{0.5})_{0.15}O₃ ceramic. After that,

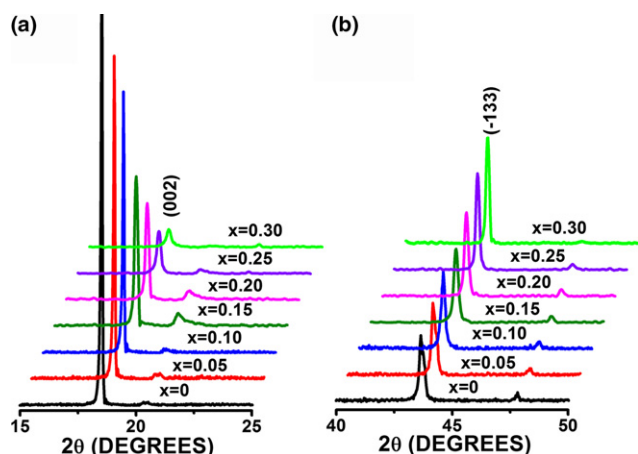


Fig. 1. The variation of (a) (002) peak and (b) (–133) peak of the Li₂Ti_{1-x}(Al_{0.5}Nb_{0.5})_xO₃ (*x* = 0–0.3) ceramics sintered at optimal temperatures for 2 h.

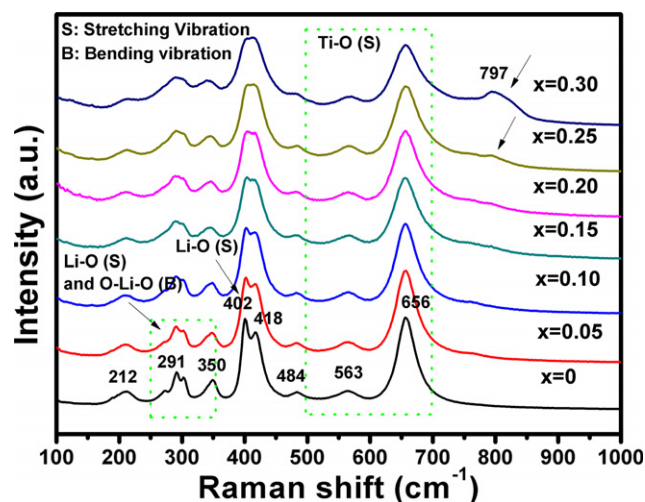


Fig. 2. The Raman spectra of the Li₂Ti_{1-x}(Al_{0.5}Nb_{0.5})_xO₃ (*x* = 0–0.3) ceramics sintered at their optimal temperatures.